Rev.Adv.Mater.Sci. 10 (2005) 215-223

HIGH PERFORMANCE GAS SENSING MATERIALS BASED ON NANOSTRUCTURED METAL OXIDE FILMS

G. Kiriakidis[1,2], M. Suchea [1,2], S. Christoulakis [1,2] and N. Katsarakis[1,3]

[1]Institute of Electronic Structure and Laser, Foundation for Research & Technology Hellas, PO Box 1527 Vasilika Vouton, 71110 Heraklion, Crete, Greece
[2]University of Crete, Physics Department, 71110 Heraklion, Crete, Greece
[3]Center of Materials Technology and Laser, School of Applied Technology, Technological Educational Institute of Crete, Heraklion, Estavromenos, 71004 Heraklion, Crete, Greece

Received: May 30, 2005

Abstract. Nanostructured InO_x and ZnO_x films and their sensing properties are presented with respect of their surface texture and composition. They were prepared by reactive dc magnetron sputtering in a mixture of argon-oxygen plasma using metallic In and Zn targets onto Corning glass and Si substrates at room temperature. The structure of the films, i.e., the crystallinity and the microstructure, was investigated by X-ray diffraction analysis and Atomic Force Microscopy (AFM). The nanostructure of their surfaces is highly controlled by the deposition parameters and the subsequent in-plain grain size and surface roughness, which, in term, control the transport properties, and thus the sensing characteristics of these films as measured by a conductometric technique. Based on conductivity changes of up to seven orders of magnitude and under selected deposition and film structure conditions their sensitivity was highly improved and pushed to bellow 10 ppb for O_3 and bellow 80 ppb for NO_2.

1. INTRODUCTION

Metal oxides such as InO_x and ZnO_x are very interesting semiconducting materials. They behave as insulators in their stoichiometric form and as highly conducting semiconductors with a wide direct optical band-gap (3-4 eV) in their non-stoichiometric form, providing high transparency in the visible light range and high reflectivity in the IR light range.

This unique combination of electrical and optical properties has led numerous researchers to a thorough investigation of the growth and characterization of thin semiconducting metal oxide films due to their obvious application as transparent electrodes in electronic and optoelectronic devices, such as solar cells, diffusion barriers in $Al/In_2O_3/Si$ structure and flat panel displays. In the last years, the gas-sensing properties of Indium and Zinc oxides as a semiconductor gas sensor have been investigated. It was found that they exhibit high sensitivity to oxidizing gases, such as NO_x [1] and O_3 [2,3], as well as to H_2 [4], and therefore can be used in detectors for these gases. It was also found that doping indium oxide with Mn^{+2} ions increases the electrical resistivity by several orders of magnitude at room temperature in a dry atmosphere, whereas the resistivity of the film decreases rapidly when brought into contact with moist air. This property has prompted some researchers to investigate a possible use of manganese-doped and other divalent-ion-doped indium oxide films as humidity sensors [5,6].

Corresponding author: G. Kiriakidis, e-mail: kiriakid@iesl.forth.gr

© 2005 Advanced Study Center Co. Ltd.

Several deposition techniques have been employed to grow polycrystalline metal oxide films of which dc and rf sputtering [7-9] are the most prominent due to the precise control of deposition conditions and reproducibility of film quality.

For all these films oxygen plays an important role since their conductivity arises from the excess electrons of charged oxygen vacancies in their structure. Accordingly, controlling the oxygen partial pressure during the deposition one may produce films with different conductivities, from the insulating transparent phase to a highly conducting transparent phase.

Over the last decade several groups reported that the electrical properties of metal oxide films depend greatly on their structure and surface characteristics and numerous studies have presented theoretical models as well as experimental results on the transport mechanisms that induce the conductivity changes as a result control their sensitivity level. However it is only recently that research has been intensified and film structural characteristics of the nano-scale are correlated with their gas sensing response. D. Zhang *et al.* [10] together with the group from the University of South California have published some of the most exiting recent results on In_2O_3 nanowire mat devices that are capable of detecting NO_2 down to 5 ppb levels. The nanowires were fabricated by laser ablation while Ti/Au electrodes were applied as electrodes on a Si/SiO_2 back gate substrate. However comparable levels of sensitivity towards NO_2 and O_3 have also recent by reported [11] for thin films of In_2O_3 with controlled nanostructured surfaces, opening up the field for the new generation of sub-ppb gas sensing devices. To this end, this work is an effort to present some of the most interesting recent results that underline the significant contribution of film nanostructure and predominately of grain boundaries over the characteristics and ultimate improvement of their sensing detection levels.

2. GRAIN BOUNDARIES AND THE CONDUCTIVITY MECHANISM IN POLYCRYSTALLINE SEMICONDUCTING FILMS

The conductivity behavior in polycrystalline films closely approaches that of semiconductors with predominant grain boundary conduction mechanism. The carrier mobility in these films is limited by scattering at the surface and grain boundaries as well as by normal bulk processes.

A model of intergrain boundaries being affected by the diffusion of an active gas has been used by Seager and Ginley [12] to explain the changes of conductivity seen initially in polycrystalline silicon and later in In_2O_3. It was observed that diffusion of oxygen down the grain boundaries promoted significant changes in the density of defect states in these regions, resulting in a decrease in conductivity. The main features of this conduction model are: conduction from grain to grain, disturbed by surface barriers, which are strongly influenced by chemisorbed oxygen. The formation of potential barriers, at the grain boundaries, was proposed by Petritz [13] as early as 1956, in addition to the normal lattice discontinuity caused by the boundaries. According to this model, grain boundary potential barriers are formed in an n-type semiconductor when the grain boundary region has a lower chemical potential (Fermi level E_F) for majority carriers, than the grains, due to the density of defect states in this region. These defect states can appear by the tendency of grain boundaries to act as diffusion sinks for impurities. Therefore, these defect states can be treated as trapping centers for majority carriers resulting in a reduction of their concentration in the boundary region. This reduction results in a flux of majority carriers into the boundary region creating a space charge build up at these boundaries, which prevents further flux of majority carriers and therefore forms a depletion region for these carriers. There are two different mechanisms by which majority carriers can cross a grain boundary potential barrier. The first is thermal emission over the barrier and the second is quantum mechanical tunneling. However in evaluating electrical characteristics of semiconducting films, it is common to compare the behavior of the films to that of the bulk crystal. If the bulk crystal was perfect, the conduction carriers could flow unimpeded in a perfect periodic potential. However, in a real bulk crystal lattice, vibrations, impurities and defects can cause deviations from the ideal behavior. The carrier mobility is then related directly to the mean free time between collisions, which in turn is determined by the various scattering mechanisms. Two scattering processes are important for bulk crystal behavior in semiconductors: lattice scattering and ionized impurity scattering. Lattice scattering results from thermal vibrations of the lattice atoms at any temperature above absolute zero. Since lattice vibration increases with increasing temperature, lattice scattering becomes dominant at high temperatures. Therefore, the mobility decreases with increasing temperature. Bar-

deen and Shockley [14] have shown that the mobility due to lattice scattering can be expressed as:

$$\mu_L = \frac{\sqrt{8\pi} g\hbar^4 C_{11}}{3E_{d\varsigma} m^{*5/2} * (KT)^{3/2}} \sim T^{-3/2},$$

where C_{11} is the average longitudinal elastic constant of the semiconductor, $E_{d\varsigma}$ is the displacement of the edge of the band per unit dilation of the lattice, m^* is the conductivity effect mass and q the carrier charge. Impurity scattering results when a traveling carrier passes near to an ionized impurity centre. The probability of impurity scattering depends on the total concentration of ionized impurities. In contrast to the lattice scattering, impurity scattering becomes less significant at high temperatures. This is due to the fact that the mean velocity of the carriers increases with temperature, with the result that the carriers remain near the ionized impurities for a shorter time. Therefore, the scattering becomes less effective. Conwell and Weisskopf [100] have shown that the mobility due to impurity scattering can be expressed as:

$$\mu_1 = \frac{64\sqrt{\pi}\varepsilon_\varsigma^2 (2KT)^{3/2}}{N_I q^3 m^{-1/2}} \left\{ \ln\left[1 + \left(\frac{12\pi\varepsilon_\varsigma KT}{q^2 N_I^{1/3}} \right)^2 \right] \right\}^{-1}$$

$$\sim N_I^{-1} T^{3/2},$$

where N_I is the ionized impurity density and ε_ς is the semiconductor permittivity.

In accordance with the grain boundary conduction model, oxygen diffuses into a polycrystalline film along grain boundaries and, from these, into the grains themselves. When a polycrystalline film is exposed in air or in an oxygen atmosphere, the grain boundaries absorb oxygen. As a result of that, the surface of the grains is covered with many adsorbed oxygen ions. By the process of chemisorption one may expect either removed majority carriers or supply majority carriers at the grains. However, when oxygen is chemisorbed on a polycrystalline film, not only the bulk effect of oxygen occurs in the grains, but the oxygen adsorbed at the grain boundaries has an additional effect on the electronic transport. As the origin for the formation of potential barriers at the grain boundaries is the existence of defect states in the boundary region, it is expected that any increase in the density of these defect states will cause an increase in the barrier height. The diffused oxygen ions act as trapping centers for the electrons in the boundary region, resulting in a reduction of their concentration. Therefore, these oxygen traps are identical to or associated with the defect states that are responsible for the charge build up at the grain boundaries. It is then believed that the barrier height at the grain boundaries is determined by the amount of chemisorbed oxygen. The bulk effect of adsorbed oxygen in polycrystalline films in terms of the band diagram is: oxygen produces a deep surface state below the conduction band, which removes one electron from the conduction band for each oxygen ion chemisorbed. Therefore, in an n-type semiconductor, the effect of oxygen is to decrease the dark conductivity, while in a p-type semiconductor, the chemisorption of oxygen contributes an additional hole to the material and increases the conductivity.

The above discussion leads to the conclusion that the grain boundaries in polycrystalline semiconducting films behave like 'sponges' absorbing oxygen and passing it on the grains. However, this process is further complicated in the case of our metal oxide films since they are not only composed solely of high quality bulk material separated by grain boundaries. The material is well known to contain stoichiometry deviations, point defects, etc. in addition to the grain boundaries, which can strongly affect the electrical properties. In the case of polycrystalline semiconducting metal oxides, point defects, which can change the stoichiometry of the material, are mainly related to oxygen. It is in the context of understanding the role of these point defects and the effect upon the film sensing characteristics that the discussion precedes in the following.

3. EXPERIMENTAL

An Alcatel dc sputtering system with a 99.999% purity target (15 cm diameter) was applied for producing our InO_x films. The depositions were carried out at a pressure of $8{\cdot}10^{-3}$ mbar in an oxygen atmosphere. The base pressure of the chamber was $\leq 5{\cdot}10^{-7}$ mbar. Corning 1737F glass substrates, which had thermally evaporated NiCr electrodes for electrical measurements were used. During the same deposition run, different substrates with electrodes omitted were coated for performing the structural and morphological characterization of these films. The substrate temperature was varied for InO_x films between room temperature (RT) and 300 °C, and the film thickness from 10 to 725 nm. The film thickness was measured in-situ by a Leybold XTM/2 quartz crystal deposition monitor and controlled after deposition with the Stylus method. In the case of dc sputtered ZnO_x thin films, the depositions were

carried out using either a 99.999% pure zinc target or a ZnO sintered ceramic target. The substrate temperature was kept at 27 °C (RT), and the film thickness at ~100 nm. In the case of the metallic target, the depositions were done for two different plasma current settings (I_1=0.44 A and I_2=0.25 A) at different Ar/O_2 concentrations. ZnO_x thin films were also deposited by Pulsed Laser Deposition (PLD) in oxygen atmosphere using a XeCl excimer laser at 308 nm.

For the structural analysis of the deposited films, X-ray diffraction (XRD) measurements were carried out using a Rigaku diffractometer with Cu K_α X-rays. The surface morphology (grain size and surface roughness) was measured with a Nanoscope III atomic force microscope using a normal silicon nitride tip (125 μm) in Tapping Mode scanning the surface with an oscillating tip to its resonant frequency (200-400 kHz). Optical microscopy characterization was done with a Leica Optical Microscope using reflection mode and different magnifications. Electron Probe Microanalysis (EPMA) and Secondary Ion Mass Spectrometry (SIMS) analyses of our InO_x thin films were performed at 'Frauenhofer Institut fuer Schicht- und Oberflaechentechnik' in Braunschweig, using CAMECA SX50 and CAMECA IMS 5f respectively. The electrical characterization was performed in a special designed reactor described elsewhere [7]. In this work, all conductivity measurements were carried out at RT in a homemade system utilizing a pencil Hg lamp for the photoreduction ('conducting' state), at FORTH and selectively at the INDOORTRON facilities at the European JRC at ISPRA in Italy. Consequently, exposing the films into well-controlled atmospheres performed oxidation. Films with different thickness ranging from 20 nm to 200 nm were also deposited onto alumina-based transducers (5 mm × 5 mm). An overview of the transducers and their specifications was presented earlier [12].

4. RESULTS AND DISCUSSION

The structure, i.e. the crystallinity and the microstructure, of the as-deposited InO_x films prepared by dc reactive magnetron sputtering at room temperature was examined using X-ray diffraction analysis and Atomic Force Microscopy {AFM}. The X-ray diffractograms exhibited a body-centred cubic (b.c.c.) structure with a_0 =1.014 ±0.006 nm, which is in good agreement with the literature value 1.0118 nm (ASTM card 6-0416). All the InO_x films exhibited a preferred orientation along the [222] axis characteristic of the sputtered films, independently of the oxygen content used in the argon -oxygen plasma during the deposition. However, indium oxide films prepared by reactive evaporation, but with varying both substrate temperature and oxygen partial pressure [15], have been reported to have a preferred orientation sometimes along the [222] axis and other times along the [400] axis, depending on these deposition parameters. On the other hand, indium oxide films deposited by spray pyrolysis [16] and at T_{pyr}> 350 °C demonstrated a predominant [100] orientation while for depositions at high temperature of pyrolysis both [400] and [222] were present. ALE is also reported to show texture of the same nature as spray pyrolysis underlining the fact that deposition parameters and techniques are predominant factors for the film texture. Similarly, for ZnO the predominant XRD peak was found to be the [002] showing a preferred growth orientation along the c-axis perpendicular to the substrate while those prepared by dc sputtering have shown a polycrystalline structure with an additional orientation along the [103] corresponding to the reflections of the wurtzite ZnO structure [17,18].

Other additional parameters that play a decisive role on the film structure are film thickness and deposition rate. These two parameters control not only the film growth structure as shown by XRD but are responsible for the film grain size and their surface roughness. G. Korotcencov *et al.* [16] have recently shown the influence of film thickness on the ratio of intensities of the main XRD peaks I(400)/I(222) for the spray pyrolysis technique while R. Martins *et al.* [19] have noted the striking differences between sputtered and spray pyrolysis ZnO films (Fig.1).

AFM study on the film surface morphology by different techniques has revealed very significant variations. Not only the film grain size and roughness was changing but also as shown in Fig. 2 the overall growth characteristics may be influenced by the applied technique and growth parameters such as growth rate, growth temperature and growth atmosphere.

As it is expected since the growth parameters and techniques control the film surface structural characteristics it is natural to expect that parameters such as conductivity and consequently for these metal oxides, sensitivity to reducing and oxidizing gas will be also effected. Indeed due to the wide interest on these metal oxides as gas sensors, their surface characteristics are directly controlling the two main surface based sensing mechanisms i.e. the Conductometric and Surface acoustic waves (SAW). Both of these techniques are

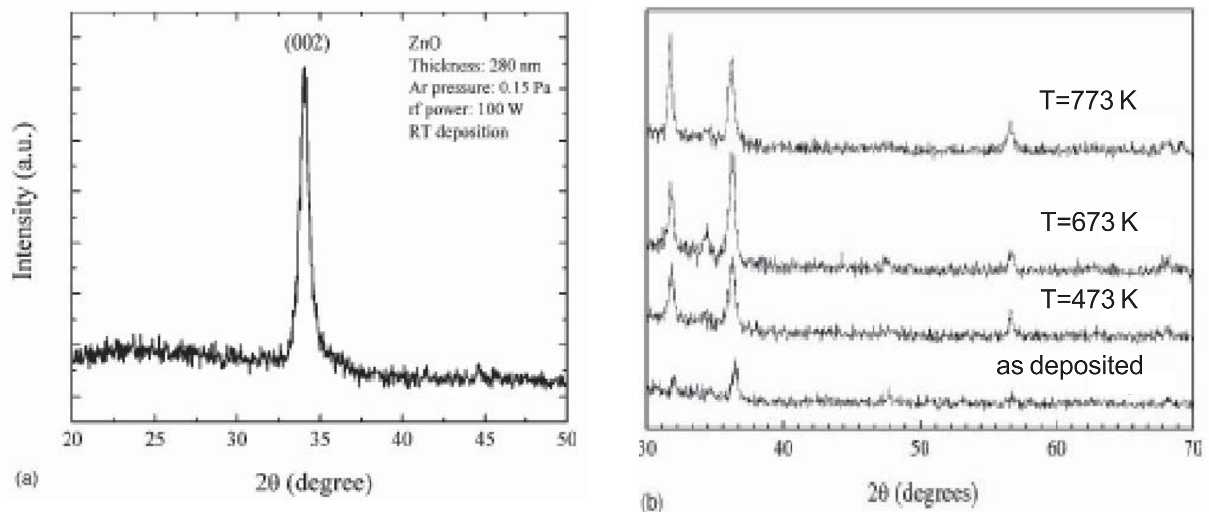

Fig. 1. XRD patterns of undoped ZnO films produced by spray pyrolysis and annealed at different temperatures as shown at the inset (a) an rf magnetron sputtering film (b).

widely applied for their reliability and reproducibility while recent results utilizing either have demonstrated the potential to improving the sensing capability of InO_x and ZnO films against volatile gases such as O_3 and NO_2 to levels bellow 1 ppb. A comparable conductometric performance of various films prepared under different temperatures by the four main techniques of sputtering, pulsed laser, evaporation and spray pyrolysis is presented in Table 1. This demonstrates the significant variations in the conductivity values that could be encountered and that correspondingly affecting the material gas sensing characteristics. It should be noted here that although most of the presently used metal oxide based sensors are currently operate at elevated temperatures, future applications will prefer those operating at room temperature (RT) due to mainly lower energy consumption.

It is because in many technological applications there is a limitation in the allowed substrate operating temperature, such as, in organic layers for electroluminescent diodes, flat panel displays, and solar cells, and thus the need for good sensing characteristics at low temperature is imminent. For films grown by dc sputtering and at RT it has been found [24] that operation at elevated temperatures not only

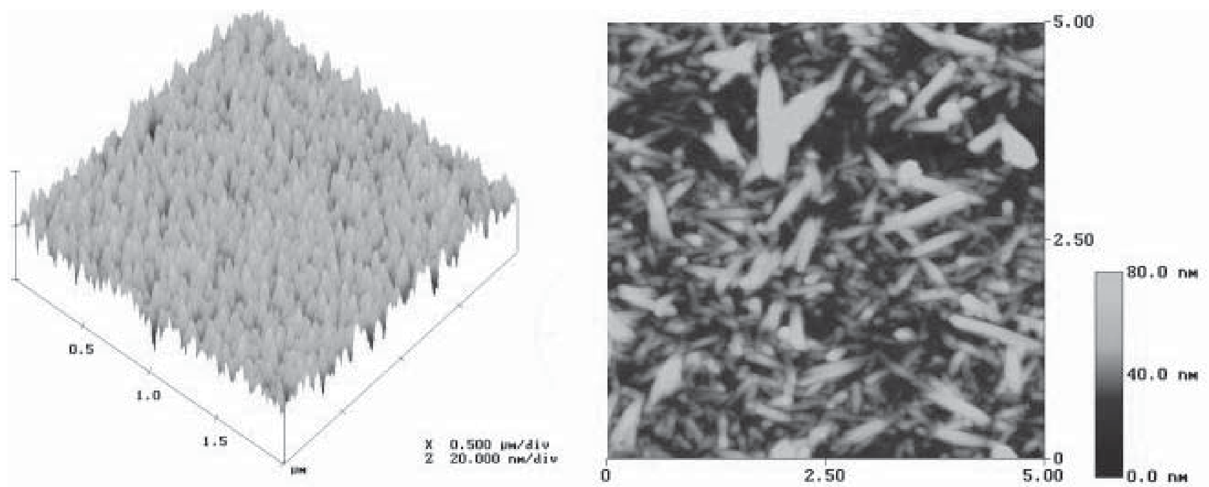

Fig. 2. Typical AFM. Images of ZnO thin film surface growth from metallic target (a) by sputtering, b) by PLD.

Table 1. Performance of the conductivities of some InO_x and doped-In_2O_3 films with the corresponding operating temperatures.

Deposition technique	Substrate	Temperature	Conductivity ($\Omega^{-1}cm^{-1}$)	Reference
Sputtering	InO_x:	RT	$1.5 \cdot 10^2$	in this work
	ZnO-InO_x	350 °C	$5 \cdot 10^3$	[20]
	ZnO-InO_x	RT	10^3	[20]
PLD	ITO	RT	$2 \cdot 10^3$	[21]
Evaporation	InO_x	0.5 °C/s	50	[22]
Spray pyrolysis	InO_x	380 °C	$7.8 \cdot 10^2$	[23]
	ITO	350 °C	$2 \cdot 10^2$	[23]

does not control to their sensitivity but on the contrary it has the opposite effect leading to a detrimental effect and a corresponding decrease of their sensing capabilities as show in Fig. 3a and 3b. Furthermore there has been demonstrated that increase in film thickness leads to a reduction of film sensing characteristics as denoted by the ration of maximum to minimum conductivities (σ_{max} / σ_{min}) during the reduction and oxidation circles. The effect was reported, a few years ago, by M. Bender *et al.* [24] who have also introduced a model that gave a satisfactory account for the involved conduction mechanism. According to their model the sensing mechanism is primarily a top surface phenomenon controlled by an upper-most film surface layer of a few nanometers while the remaining film thickness is only contributing to an additional resistance thus reducing the measured film conductivity. That model was recently confirmed by high resolution SIMS depth-profiling analyses showing indeed that any oxygen deficiency on the film surface is confined to the top 5-6 nm (Fig. 4.).

Since the electrical properties are directly related to the sensing response of these films, and in view of the critical role of the operating temperature upon the new generation of gas sensors, one should focus on those parameters that would maximize sensitivity while maintaining a low temperature operation. The study of the conductometric behavior of films grown at RT with thickness from 34 to 270 nm at the temperature range from RT to 200 °C has shown [11] a distinct sensitivity to the operating temperature. Recent results shown in Fig. 5 demonstrate the dramatic increase of the current flow

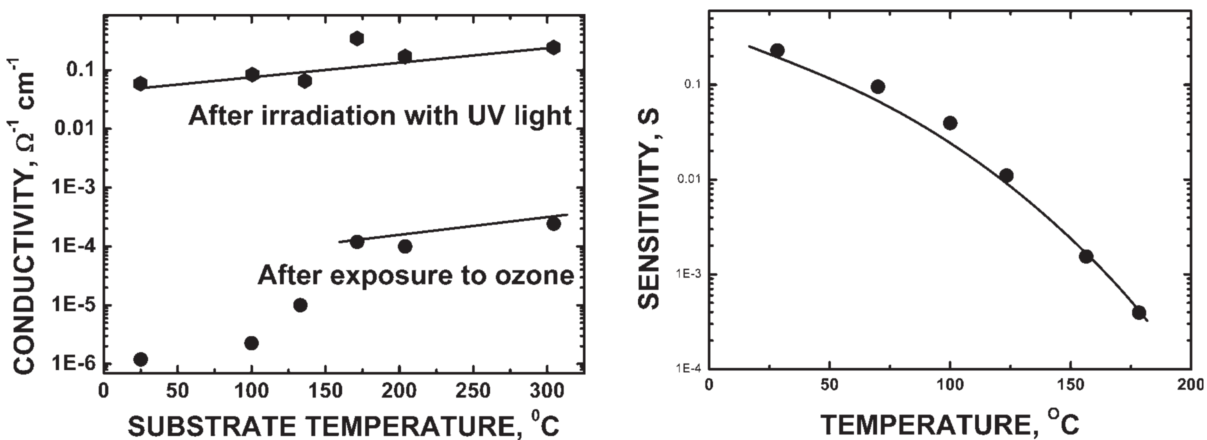

Fig. 3. **a)** Maximum and minimum conductivities of InO_x films deposited at different substrate temperatures, b) Sensitivity of a 100 nm thick InO_x film vs. temperature.

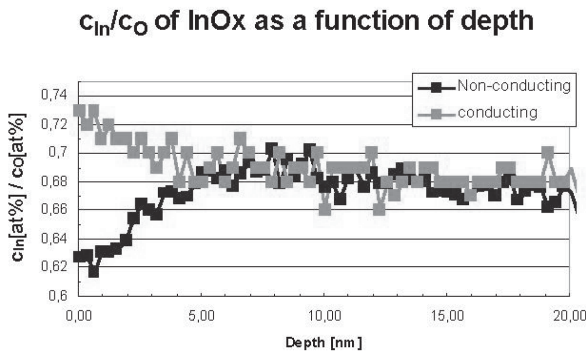

Fig. 4. In:O atomic ratio as a function of depth in the near-surface region derived from SIMS-depth profiles.

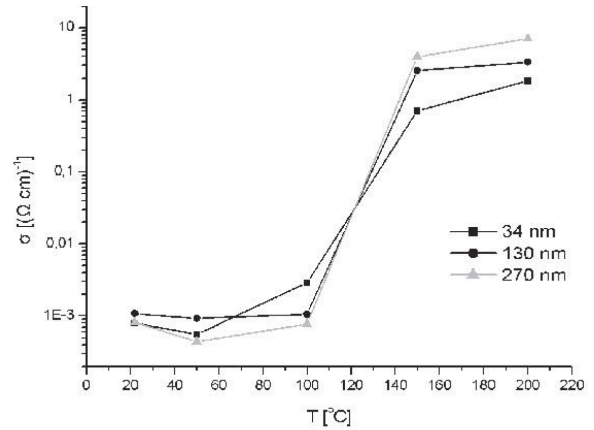

Fig. 5. Conductometric response of sputtered InO_x films as a function of operating temperature.

through the film in its insulating state (σ_{min}) of more than three orders of magnitude and the existence of a transition temperature between 100 and 200 °C. These results confirm earlier observations [19,24,25] and are attributed to structural changes in the film at temperatures beyond 100 °C, believed to be related to grain size increase observed by AFM, with parallel partial annihilation of oxygen vacant sides, reduction in the film defect density and increase of its stoichiometry. Films operating below 100 °C exhibit an enhanced sensitivity denoted as σ_{max} / σ_{min} in line with previous conductometric studies on sputtered films.

InO_x thin films deposited onto alumina-based transducers were also exposed to a sequence of air (20 °C & 40%RH) and 10-minute ozone pulses with concentrations of 50 and 150 ppb at RMIT Melbourne. At room temperature these sensors had a time-dependent response; they did not reach equilibrium within the 10-minute gas exposure. However, the films had a stable response of up to 7, towards a 50 ppb O_3 concentration at room temperature. At 50 °C, the 50 nm thickness film had an O_3 response of 10, while the 20 nm film had a maximum response magnitude of 13 at an operating temperature of 100 °C (Fig. 6). As it can be seen from Fig. 6, each film

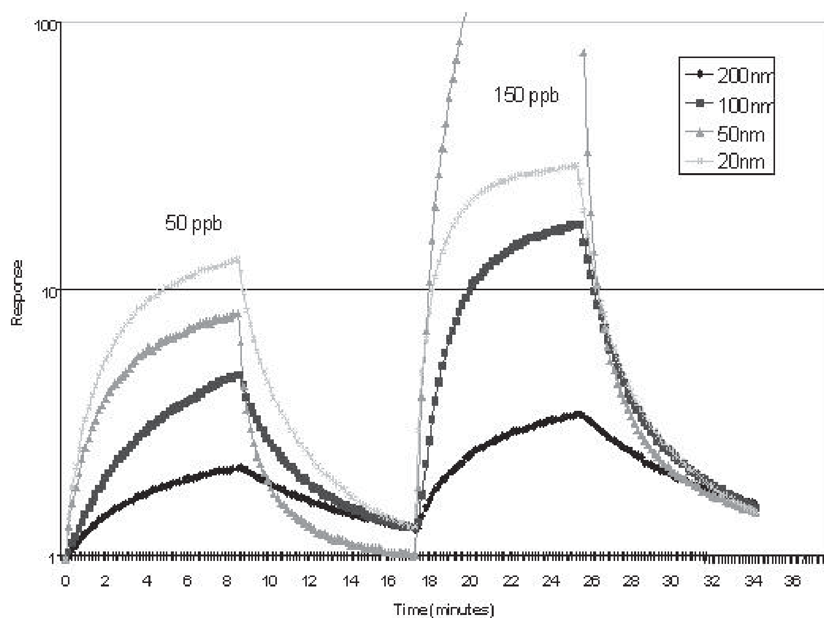

Fig. 6. The dynamic response of the InO_x films towards O_3 at an operating temperature of 100 єC.

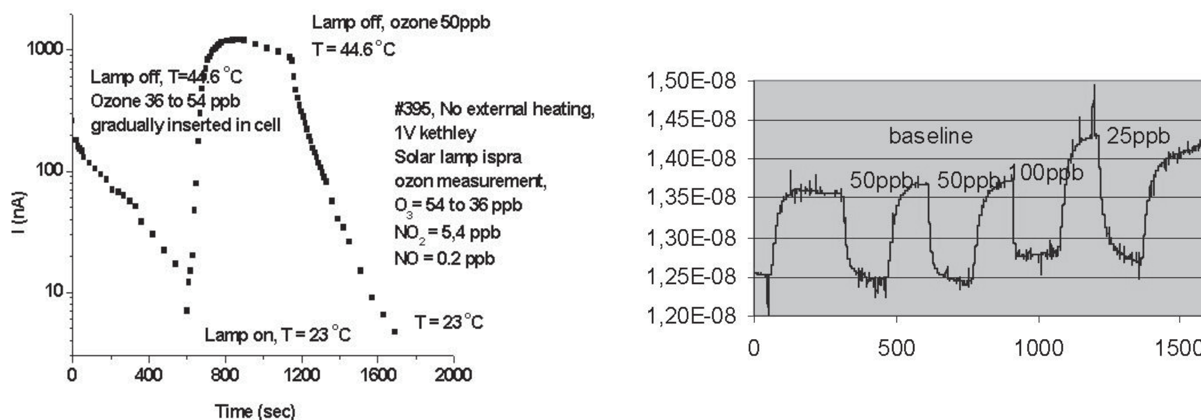

Fig. 7. a) Conductometric response of a 100 nm sputtered film at O_3 concentrations of 36-50 ppb, b) SAW response analysis.

thickness exhibited a characteristic sensitivity confirming earlier conductometric results discussed above [11-14]. Moreover, it is demonstrated that our dc sputtered InO_x films responded to O_3 concentrations well bellow 50 ppb at low operating temperatures ranging from 100 °C to RT, showing their potential for further improvement.

Fig. 7a shows a typical conductometric response of our films at low temperature (23-45 °C) and at O_3 concentrations ranging from 36 to 54 ppb. Photoreduction was achieved utilizing a solar spectrum-simulating lamp with UV cut-off radiation at 280 nm. The presence of other volatile gases was also monitored and were restricted to <5 ppb for NO_2 and < 1 ppb for NO. Under the above conditions the films have shown a remarkable response to O_3 of more than two orders of magnitude confirming our expectations for ultra low sensing applications at low *T*. Parallel studies utilizing the SAW technique have demonstrated the potential for thin films to achieving ultra low sensing performances down to below one ppb levels and thus stay competitive with the emerging nanorod / nanowire [10] technologies.

5. CONCLUSIONS

We reviewed the gas sensing properties of InO_x thin films deposited by dc sputtering and ZnO_x thin films deposited both by dc sputtering and PLD. The sensitivity of the films towards ozone correlated with the deposition parameters like film thickness, substrate deposition temperature, growth rate etc was presented. SIMS analysis has shown that InO_x films in the 'conducting' state i.e., after UV illumination, show a deficit of oxygen in the top 5 nm, which could be responsible for the conductivity increase of the UV exposed samples. Conductometric measurements as well as resent tests on SAW devices with InO_x film as selective layer show high sensitivity levels towards O_3 below 25 ppb. It is believed that these films are candidates for the detection of ozone and NO_2 at very low levels down to1 ppb.

ACKNOWLEDGEMENTS

The authors are grateful for the EU financial support through the projects 3rd Gen LAC No NNE5-2001-00961and ASSEMIC No 504826. He also acknowledges the contributions collaborators at FORTH and at the Technological Educational Institute of Crete as well as the teams at Melbourne, Braunschweig and ISPRA for valuable analyses and tests.

REFERENCES

[1] A. Gurlo, M. Ivanovskaya, A. Pfau, U. Weimar and W. Göpel // *Thin Solid Films* **307** (1997) 288.

[2] T. Takada, K. Suzuki and M. Nakane // *Sensors and Actuators B* **13-14** (1993) 404.

[3] T. Takada, H. Tanjou, T. Satio and K. Harrada // *Sensors and Actuators B* **24-25** (1995) 548.

[4] Y. Yasukawa, T. Seki, J. Muramatsu, S. Sugie, S. Tasaka and N. Inagaki // *Sensors and actuators B* **13-14** (1993) 613.

[5] Y. Takahashi, R.B.H. Tahar, K. Shimaoka, T. Ban and Y. Ohya // *Trans. Mater. Res. Soc. Jpn.* **20** (1996) 538.

[6] R.B.H. Tahar, T. Ban, Y. Ohya and Y. Takahashi // *J. Am. Ceram. Soc.* **81** (1998) 321.

[7] C. Xirouchaki, G. Kiriakidis, T.F. Pedersen and H.Fritzsche // *J.Appl.Phys.* **79** (1996) 9349.

[8] H.K. Müller // *Phys. Stat. Sol.* **27** (1968) 733.

[9] V.M. Vainstein and V.I. Fistul // *Sov. Phys. Sem.* **4** (1971) 1278.

[10] D. Zhang, Z. Liu and C. Zhou // *Mater. Res. Symp. Proc*. **828** (2005) A2.7.1.

[11] G. Kiriakidis, *MRS Fall meeting, Symp.2, Boston 2004.*

[12] C.H. Seager and D.S. Ginley // *Appl. Phys. Lett.* **34** (1979) 337.

[13] R.L. Petritz // *Phys. Rev.* **104** (1956) 1508.

[14] J. Bardeen and W. Shockley // *Phys. Rev.* **80** (1950) 72.

[15] K.G. Copchandran, B. Joseph, J.T. Abraham, P. Koshy and V.K. Vaidyan // Vacuum **48** (1997) 547.

[16] G. Korotcenkov, V. Brinzani, A. Cerneavschi, M. Ivanov, V. Golovanov, A. Cornet, J. Morante, A. Cabot and J. Abriol // *Thin Solid Films* **460** (2004) 315.

[17] M. Suchea, S. Christoulakis, M. Katharakis, N. Katsarakis, E. Koudoumas and G. Kiriakidis, *NN2005, Crete, Greece*.

[18] M. Suchea, S. Christoulakis, K. Moschovis, N. Katsarakis and G. Kiriakidis, NN2005, Crete, Greece.

[19] R. Martins, E. Fortunato, P. Nunes, I. Ferreira, A. Marques, M. Bender, N. Katsarakis, V. Cimalla and G. Kiriakidis // *J. Appl. Physics* **96** (2004) 1398.

[20] T. Minami, T. Kakumu, Y. Takeda and S. Takata // *Thin Solid Films* **290** (1996) 1.

[21] F.O. Adurodija, H. Izumi, T. Ishihara, H. Yoshioka and M. Motoyama // *Materials Solar Cells* **71** (2002) 1.

[22] M. Girtan, G.I. Rusu, G.G. Rusu and S. Gurlui // *Appl. Surf. Sci.* **162-163** (2000) 492.

[23] J.J. Prince, S. Ramamurthy, B. Subramanian, C. Sanjeeviraja and M. Jayachandran // *Journal of Crystal Growth.* **240** (2002) 142.

[24] M. Bender, N. Katsarakis, E. Gagaoudakis, E. Hourdakis, E. Douloufakis, V. Cimalla and G. Kiriakidis // *J. Appl. Phys.* **90** (2001) 5382.

[25] V.D. Das, S. Kirupavathy, L. Damodare and N. Lakshminarayan // *J. Appl. Phys.* **79** (1996) 8521.